Vibration-Rotation Coupling in a Quasilinear Symmetric Triatomic Molecule

Jae Shin Lee

Department of Chemistry College of Natural Sciences Ajou University Suwon 441-749
Received October 15, 1993

The effect of the vibration mode coupling induced by the vibration-rotation interaction on total energy was investigated for the states with zero total angular momentum($J=0$) in a quasilinear symmetric triatomic molecule of AB_2 type using a model potential function with a slight potential barrier to linearity. It is found that the coupling energy becomes larger for the levels of bend and asymmetric stretch modes and smaller for symmetric stretch mode as the excitation of the vibrational modes occurs. The results for the real molecule of CH_2^+, which is quasilinear, generally agree with the results for the model potential function in that common mode selective dependence of coupling energy is exhibited in both cases. The differences between the results for the model and real potential function in H-C-H system are analyzed and explained in terms of heavy mixing of the symmetric stretch and bend mode in excited vibrational states of the real molecule of CH_2^+. It is shown that the vibrational mode coupling in the potential energy function is primarily responsible for the broken nodal structure and chaotic behavior in highly excited levels of CH_2^+ for $J=0$.

Introduction

Mode mixing in highly excited vibrational states of polyatomic molecules is an important and intriguing problem for molecular theorists. In the lower states of internal energy, the separation of vibrational modes can be done effectively, for example, using normal mode technique based on harmonic approximation of the potential energy surface and restricted kinetic motion of nuclei. It is possible to characterize and assign these states by the specific vibrational mode involved. In highly excited states, however, the assumption of potential harmonicity and small amplitude motion of nuclei usually breaks down and the coupling between various vibrational modes begins to have significant effect on molecular motions and energies. Vibrational mode coupling can be induced by the potential anharmonicity and kinetic vibration-rotation interaction like centrifugal distortion and Coriolis interaction. Experimentally, vibrational mode coupling and vibration-rotation interaction in polyatomic molecules are responsible for various spectroscopic phenomena like Fermi resonance and l-type doubling, and also play an important role in understanding the quantum correspondence of classical chaos in highly excited states.[13]

In last ten years or so, there has been tremendous progress toward developing effective formalisms for obtaining exact energies and wavefunctions in these high energy regime.[4-6] However, regardless of whatever formalism or methodology used for the calculation of energies and wavefunctions, it is always necessary to have a genuine potential energy surface to correctly understand the dynamics of the molecules. The *ab initio* potential energy surface is the most ideal and desirable one for any kind of dynamics calculations for the motion of nuclei, but it still is a very expensive and difficult task to obtain enough *ab initio* potential points with desired accuracy for most polyatomic systems.

In a recent paper, Natanson pointed out that significant errors could be introduced by the neglect of vibrational mode coupling terms of the potential energy function in the calculation of total energy of the triatomic system.[7] The vibrational mode coupling terms in kinetic energy operator are usually considered to make insignificant contributions to the total energy in the lower levels and the contributions are expected to increase as the levels go higher for most polyatomic systems. However, the effects of kinetic vibrational mode coupling in high energy region are yet to be examined.

In this paper, we study the effects of vibrational mode coupling terms in kinetic energy operator on the total energy in their excited vibrational states with zero total angular momentum ($J=0$) in a quasilinear symmetric triatomic molecule of AB_2 using the model potential function, which has a slight potential barrier to linearity from equilibrium bent geometry. In section II we introduce the basic theoretical method for vibrational calculations involved. In section III we compare potential surfaces of the model potential function with those of the real molecular potential function and discuss the reliability of the model potential function. The details of calculations are explained in sec. IV, and the results for model potential functions are discussed and compared with the results of vibrational calculations for real molecule of CH_2^+ in sec V. The summary and conclusion are in section VI.

Theoretical Method

The adiabatic vibration-rotation Hamiltonian operator of a polyatomic molecule can be derived using various coordinate systems, depending on specific problems involved. Since the model potential for a triatomic molecule is developed in an arbitrary vibrational coordinate system defined from a reference linear configuration, the Hamiltonian operator derived in the same internal coordinate system is used to obtain the eigenvalues and eigenvectors for the vibration-rotation Schrödinger equation of a symmetric triatomic molecule.[8] The general transformation equation from a space-fixed cartesian coordinate system to a molecule-fixed coordinate system for an N-atom molecule is given as

$$R_n = R_0 + S^{-1}(\alpha\beta\gamma)(r_n^{eq} + 1^{(n)}\eta) \qquad (n = 1,2,\cdots,N)$$

Here R_n and R_0 is the position vector and center of mass vector in the space-fixed cartesian coordinates system, respectively, while r_n^{eq} is the constant vector representing the equilibrium position of the n-th atom in the molecule fixed axis system. $S(\alpha\beta\gamma)$ is the 3×3 matrix which rotates the space-fixed axis system by Euler angles α, β, and γ into the molecule-fixed axis system, and $1^{(n)}$ is the $3\times(3N-6)$ matrix whose element, $1^{(n)}_{ij}$ determines the amplitude of the displacement of n-th atom along the $i(i=x, y, z)$ molecule-fixed axis by the vibrational coordinate η_j.

For the case of a symmetric triatomic molecule, A-B-C with A=C, we choose the following vibrational coordinates.

$$(r_A^{eq} + 1^{(A)}\eta) = \begin{bmatrix} \frac{m_B}{2m_A}\eta_b \\ 0 \\ -r^0 - \frac{1}{2}\eta_s + \frac{m_B}{2m_A}\eta_a \end{bmatrix}$$

$$(r_B^{eq} + 1^{(B)}\eta) = \begin{bmatrix} -\eta_b \\ 0 \\ -\eta_a \end{bmatrix}$$

$$(r_C^{eq} + 1^{(C)}\eta) = \begin{bmatrix} \frac{m_B}{2m_A}\eta_b \\ 0 \\ r^0 + \frac{1}{2}\eta_s + \frac{m_B}{2m_A}\eta_a \end{bmatrix}$$

Here, r^0 is the distance between atom A and atom B in the linear reference configuration, and m_A and m_B are the masses of atom A and B. η_s, η_a and η_b represent the symmetric stretch, asymmetric stretch, and bend mode respectively. This choice of vibrational coordinate system confines the internal molecular motion in the body-fixed xz plane and the body-fixed z axis becomes the figure axis of the molecule.

The vibration-rotation Hamiltonian in this coordinate system is written as[8]

$$H = H_0 + T_{V-R}$$

where

$$H_0 = -\frac{1}{m_A}\frac{\partial^2}{\partial\eta_s^2} - \frac{m_A}{m_B M}\frac{\partial^2}{\partial\eta_a^2} - \frac{m_A}{m_B M} \times \left(\frac{\partial^2}{\partial\eta_b^2} + \frac{1}{\eta_b}\frac{\partial}{\partial\eta_b} + \frac{1}{\eta_b^2}\frac{\partial^2}{\partial\gamma^2}\right) + V(\eta_s, \eta_a, \eta_b)$$

and

$$T_{V-R} = \frac{1}{m_A(2r^0+\eta_s)^2} \times \left[J^2 - J_Z^2 - \eta_a^2\left\{\frac{\partial^2}{\partial\eta_b^2} + \frac{1}{\eta_b}\frac{\partial}{\partial\eta_b} + \frac{1}{\eta_b^2}\frac{\partial^2}{\partial\gamma^2}\right\} + \eta_b\frac{\partial}{\partial\eta_b} - \eta_b^2\frac{\partial^2}{\partial\eta_a^2} + 2\eta_a\frac{\partial}{\partial\eta_a} + 2\eta_a\eta_b\frac{\partial^2}{\partial\eta_a\partial\eta_b}\right] + \frac{1}{m_A(2r^0+\eta_s)^2} \times \left[J_+\left\{\eta_a\left(-\frac{i}{\eta_b}\frac{\partial}{\partial\gamma} - \frac{\partial}{\partial\eta_b}\right) + \eta_b\frac{\partial}{\partial\eta_a}\right\} + J_-\left\{\eta_a\left(-\frac{i}{\eta_b}\frac{\partial}{\partial\gamma} + \frac{\partial}{\partial\eta_b}\right) - \eta_b\frac{\partial}{\partial\eta_a}\right\}\right]$$

The Hamiltonian was expressed in two parts, H_0 and T_{V-R}. H_0 is the unperturbed (pure) vibrational Hamiltonian including the potential energy function, and T_{V-R} acccounts for the vibration-rotation interaction in the kinetic energy operator caused by the centrifugal distortion and Coriolis interaction. J and J_z are the total angular momentum operator and its body-fixed z component which can be expressed in terms of the Euler angles, and J_+ and J_- are the raising and lowering operators for the total angular momentum around the body-fixed z axis, respectively. M represents the total mass ($M=2m_A+m_B$), and V is the potential energy function.

The wavefunction, which is chosen to be an eigenfunction of the total angular momentum operator and its space-fixed z component, was expanded using the following basis functions.

$$\Psi^{JM} = \sum_{sabk} C_{sabk} D^J_{MK}(\alpha\beta\gamma)\Phi_s(\eta_s)\Phi_a(\eta_a)\Phi_{bK}(\eta_b)$$

Here, $D^J_{MK}(\alpha\beta\gamma)$ is the rotation matrix element with M and K representing the quantum number of space-fixed and body-fixed component of the total angular momentum, respectively. The vibrational basis function for symmetric and asymmetric stretch mode was chosen to be an eigenfunction of the one-dimensional harmonic oscillator, while the radial part solution of two-dimensional harmonic osillator eigenfunction was used for the bend mode.

Model Potential for a Quasilinear Symmetric Triatomic Molecule

Using the power expansion of the appropriate function of internal vibrational coordinates defined in Sec. II, we have developed the model potential function which can produce an arbitrary potential barrier when molecular configuration changes from bent equilibrium to linear saddle point geometry for general symmetric triatomic molecules. The model potential function is expanded as

$$V(\eta_s, \eta_a, \eta_b) = c_s f_s^2 + c_a f_a^2 + x_1 f_b^2 + x_2 f_b^4 + x_3 f_s f_b^2$$

where

$$f_s = \frac{1-\exp(-k_1\eta_s)}{k_1}, \quad f_a \frac{\tanh(k_2\eta_a)}{k_2} \quad f_b = \frac{\tanh(k_3\eta_b)}{k_3}$$

c_s and c_a are related to symmetric and asymmetric harmonic frequencies of the molecule, and they are given initially with the equilibrium geomtetry and linear reference geometry. Masses of center and end atoms are also given as the vibrational coordinates are expressed in mass weighted coordinate system. k_1, k_2, k_3 are the parameters which are optimized for the model potential function to give the reasonable behavior along the vibrational coordinates. The expansion coefficients for the pure bend terms, x_1, x_2, and symmetric stretch-bend mode mixing term, x_3, are determined from the conditions which the model potential function should satisfy. If the potential barrier height from equilibrium bent to linear reference geometry of the molecule are represented as V_0 with η_s^0, η_a^0, η_b^0 indicating the vibrational coordinates at equilibrium position of the molecule (η_a^0 was set to zero for convenience), then it holds that

$$\left(\frac{\partial V}{\partial\eta_s}\right)_{\eta_s^0\ \eta_a^0\ \eta_b^0} = 0, \qquad \left(\frac{\partial V}{\partial\eta_b}\right)_{\eta_s^0\ \eta_a^0\ \eta_b^0} = 0,$$

Table 1. Expansion Coefficients for the Model Potential Function of H-C-H with Barrier Height to Linearity of 1000 cm^{-1}

Potential parameter	$s=0.8$ $b=6.0$ $a=1.4$	
Equilibrium configuration[a]	$r_e=1.07$ Å $\theta_e=136°$	
Linear reference configuration[b]	$r^0=1.065$ Å	
Expansion Coefficient[c]	c_s	0.3484798
	c_a	65.17453
	x_1	−2.965045
	x_2	1364.669
	x_3	35.06913

[a] r_e is the equilibrium bond length between atom C and atom H. [b] r^0 is the bond length between atom C and atom H in the linear saddle point geometry. [c] In units of (Å)^n, where $n=2$ for c_s, c_a, x_1; $n=4$ for x_2; and $n=3$ for x_3.

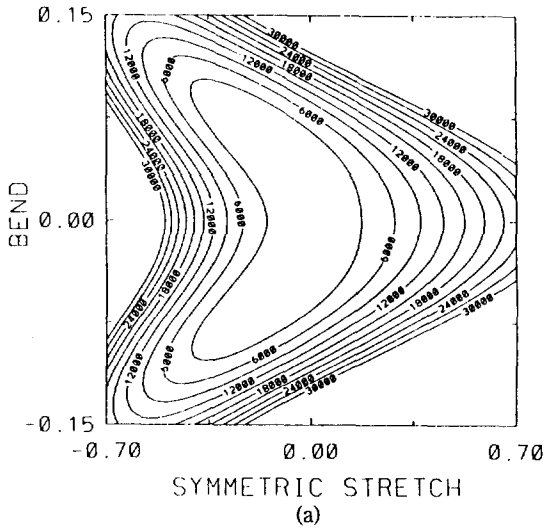

Figure 1. Contour plots of the model potential function in the (a) symmetric stretch-bend coordinate for $\eta_a=0$ and (b) asymmetric stretch-bend coordinate for $\eta_s=0$. The energy and mass weighted vibrational coordinate are in units of cm^{-1} and Å, respectively, in all figures. The interval between contour lines is 3000 cm^{-1}. The contours are drawn above the minimum of the potential.

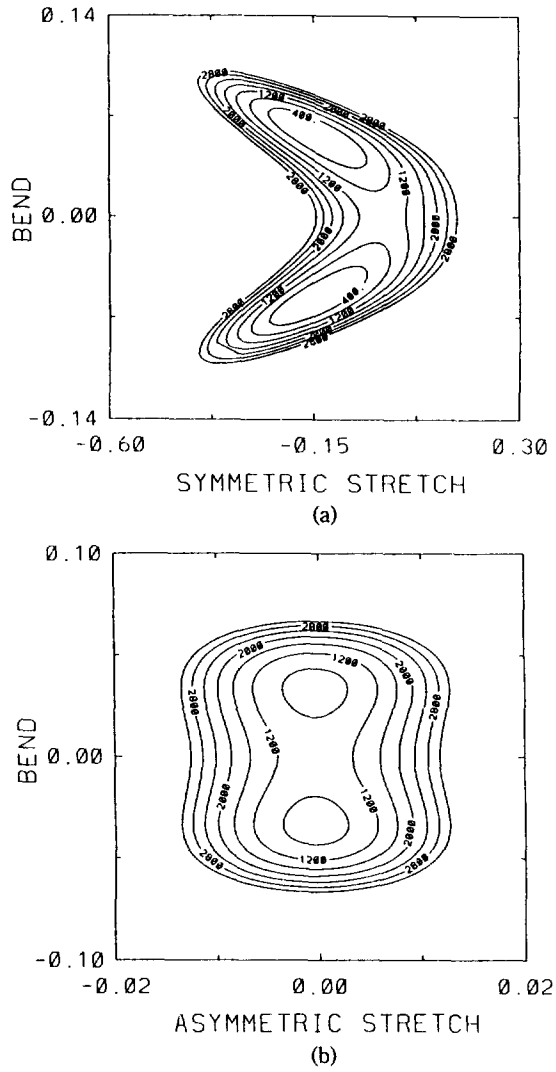

Figure 2. Contour plots of the model potential function near molecular equilibrium configuration in the (a) symmetric stretch-bend coordinate for $\eta_a=0$ and (b) asymmetric stretch-bend coordinate for $\eta_s=0$. The interval between contour lines is 400 cm^{-1}. The contours are drawn above the minimum of the potential.

$$V(\eta_s^0,\ \eta_a^0,\ \eta_b^0)=-V_0$$

In Table 1, we show the data for the model potential function generated by this method for H-C-H system with barrier height of 1000 cm^{-1}, which almost corresponds to the value of the potential barrier height of real molecule CH_2^+. Though the potential function obtained in this way is an oversimplified model of the potential surface for the real symmetric triatomic molecule, it shows physically reasonable behavior in the bound state region. In Figure 1 and Figure 2, we plot the surfaces of model potential function in the symmetric stretch and bend coordinates for $\eta_a=0$ and in the asymmetric stretch and bend coordinate for $\eta_s=0$. The double wells develop along the bend coordinate, which correspond to two bent equilibrium geometries of the molecule. There were no spurious wells or holes in the surface which could lower the energies when a large basis set is used in calculation, even in the region far from equilibrium. In Figure 3

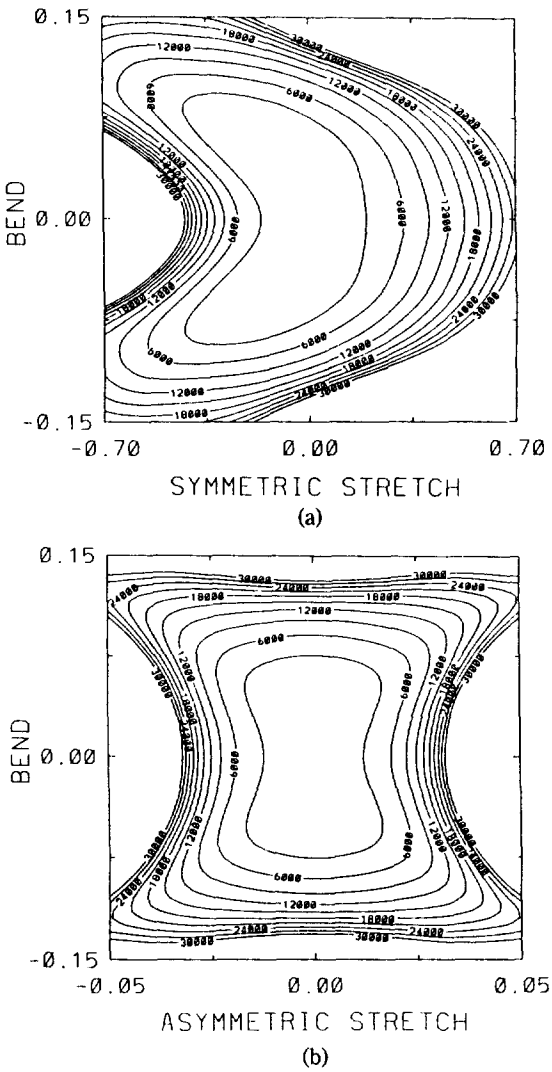

Figure 3. Contour plots of the real potential function for CH_2^+ in the (a) symmetric stretch-bend coordinate for $\eta_a=0$ and (b) asymmetric stretch-bend coordinate for $\eta_s=0$. The interval between contour lines is 3000 cm^{-1}. The contours are drawn above the minimum of the potential.

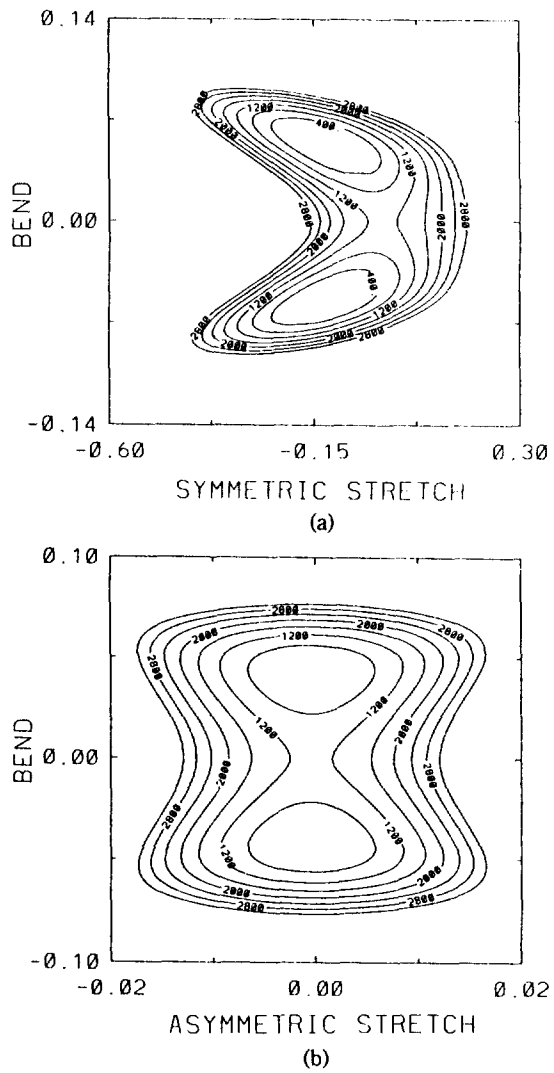

Figure 4. Contour plots of the real potential function for CH_2^+ near molecular equilibrium configuration in the (a) asymmetric stretch-bend coordinate for $\eta_a=0$ and (b) asymmetric stretch-bend coordinate for $\eta_s=0$. The interval between contour lines is 400 cm^{-1}. The contours are drawn above the minimum of the potential.

and Figure 4, same surfaces of the real potential function for CH_2^+ are shown for comparison. The real potential function for CH_2^+ was obtained by fitting the *ab initio* points[10] using the Simons-Parr-Finlan(SPF) type expansion variables.[11] The expansion coefficients and detailed features for the real potential function of CH_2^+ are given elsewhere.[12] In spite of their differences in the region far from equilibrium, similar behaviors are shown for model and real potentials in the physically important region. These were some of the contour plots for the model potential which assured us the validity of the potential function used to study the effects of vibration-rotation interaction on the total energy for bound states in a quasilinear symmetric triatomic molecule.

Vibrational Calculation

Using the model potential function developed in Sec. III, the vibration-rotation variational calculations were carried out with and without the vibration-rotation coupling terms (T_{V-R}) in the kinetic energy operator to investigate the effect of coupling terms on total energy for $J=0$ case in a quasilinear symmetric triatomic H-C-H system. For this molecule, since ^1H is a fermion with nuclei spin of 1/2, the total wavefunction must be antisymmetric with respect to the interchange of hydrogen atoms. The interchange has an effect of transforming the basis function as follows[13]

$$\hat{I}\{D^J_{MK}\Phi_s(\eta_s)\Phi_a(\eta_a)\Phi_{bK}(\eta_b)\} = (-1)^{J+a}D^J_{M-K}\Phi_s(\eta_s)\Phi_a(\eta_a)\Phi_{bK}(\eta_b)$$

where $\hat{I}$ is an interchange operator. Therefore, for $J=0$, basis functions of odd asymmetric stretch quantum number are connected to nuclear triplet state, while basis functions of even asymmetric stretch quantum number are connected to nuclear singlet state.

In both cases (with and without vibration-rotation coupling terms) the energies of the first 15 states from the ground

Table 2. Vibrational Energy Levels[a] for the Model Potential Function of the H-C-H System

Vibrational state[b]	E	E_0[c]	E-E_0
(0 0 0)	3991.37	3919.36	72.01
(0 1 0)	700.34	690.66	9.68
(0 2 0)	1608.74	1559.76	48.98
(0 3 0)	2708.80	2622.52	86.28
(0 4 0)	3933.10	3811.07	122.03
(0 5 0)	5246.37	5088.82	157.55
(0 6 0)	6626.84	6429.41	197.43
(0 7 0)	8060.41	7836.21	224.20
(1 0 0)	3501.59	3531.76	−30.17
(2 0 0)	6858.34	6904.52	−46.18
(3 0 0)	10117.63	10171.76	−54.13
(0 0 1)	3537.20	3399.20	138.00
(0 0 2)	7050.51	6797.62	252.89
(0 0 3)	10545.72	10195.24	350.48
(1 1 0)	4283.64	4281.12	2.52
(1 2 0)	5329.33	5288.96	40.37
(1 3 0)	6534.78	6463.71	71.07
(1 4 0)	7846.49	7731.63	114.86
(1 5 0)	9235.38	9085.26	150.12
(0 1 1)	4271.54	4089.87	181.67
(0 2 1)	5257.44	4958.97	298.47
(0 3 1)	6429.43	6021.73	407.70
(1 0 1)	6988.65	6930.97	57.68
(1 1 1)	7841.31	7680.33	160.98
(1 2 1)	8960.67	8688.17	272.50

[a] All excited levels are above the ground state energy in each case of E and E_0, in units of cm^{-1}. [b] Vibrational quantum number assignment is (sym, bend, asym). [c] E_0 is the energy obtained from unperturbed Hamiltonian (H_0).

Table 3. Vibrational Energy Levels[a] for Real Molecule of CH_2^+

Vibrational state[b]	E	E_0	E-E_0
(0 0 0)	3552.69	3475.92	76.77
(0 1 0)	838.81	849.79	−10.98
(0 2 0)	1738.51	1729.56	8.95
(0 3 0)	2864.70	2831.97	32.73
(0 4 0)	4151.32	4095.73	55.59
(0 5 0)	5523.72	5449.28	74.44
(0 6 0)	6949.32	6870.02	79.30
(0 7 0)	8386.28	8313.55	72.73
(1 0 0)	2938.02	2938.71	−0.69
(2 0 0)	5858.08	5857.56	0.52
(3 0 0)	8848.93	8843.23	5.70
(0 0 1)	3227.50	3033.13	194.37
(0 0 2)	6659.53	6206.40	453.12
(0 0 3)	10416.65	9611.72	804.92
(1 1 0)	3756.83	3767.84	−11.01
(1 2 0)	4645.52	4636.08	9.45
(1 3 0)	5769.12	5734.92	34.21
(1 4 0)	7085.04	7020.98	64.06
(1 5 0)	8610.70	8537.69	73.01
(0 1 1)	4068.64	3904.83	163.81
(0 2 1)	4991.21	4729.54	261.68
(0 3 1)	6326.68	5745.02	581.67
(1 0 1)	6121.88	5950.12	171.76
(1 1 1)	6980.01	6799.32	180.69
(1 2 1)	8383.88	7618.38	765.50

[a] All excited levels are above the ground state energy in each case of E and E_0, in units of cm^{-1}. [b] Vibrational quantum number assignment is (sym, bend, asym). [c] E_0 is the energy obtained from unperturbed Hamiltonian (H_0).

state, which included most of the levels examined, were converged to the point that adding a further function changes the value by less than about 0.5 cm^{-1}. The typical number of basis function with this degree of convergence was 500-800. More basis functions were needed for the case of real molecule of CH_2^+ compared to the case of model potential to achieve the same convergence. Calculations were carried out on CRAY-2/UNICOS in System Engineering Research Institute(SERI) and CRAY-YMP/UNICOS in the National Center for Supercomputing Applications(NCSA) in Urbana, U.S. A.

Results and Discussion

In Table 2, we give the vibration-rotation energies with and without coupling terms in the kinetic energy operator for the model potential function. It is shown that inclusion of the vibration-rotation coupling terms increases the total energy of the molecule. However, the effect of coupling terms on total energy are quite different, depending on the vibrational mode of the state involved. While the energy difference, E-E_0, becomes bigger for the bend and asymmetric stretch mode as the excitation occurs, it becomes smaller for the excitation of symmetric stretch mode. There is a clear distinction in the effects of the kinetic vibration-rotation coupling terms on total energy according to the excited modes of the vibrational states.

The decrease of the energy difference between E_0 and E in the states of the symmetric stretch excited mode could be understood by examining the symmetric stretch coupling term in the kinetic energy operator, which appears only in centrifugal distortion interaction term for $J=0$ case. Since the average bond distance, $2r^0+\eta_s$, would increase as the molecule gets excited in the symmetric stretch mode,[14] the energy spacing between two successive symmetric stretch excited levels, that is, (n 0 0) and ($n+1$ 0 0), would decrease as the energy levels go higher if the energies of these states are not affected appreciably by the kinetic coupling terms of other vibrational modes than symmetric stretch mode. The mode selective dependence of the vibrational coupling effect on energy is also shown in the combination levels. For example, inclusion of the kinetic vibrational coupling terms in the Hamiltonian almost do not change the total energy from the unperturbed energy E_0 (above the difference of zero point energies) for (1 1 0) state (E-E_0 is only 2.52 cm^{-1}), while about 180 cm^{-1} of energy increase is observed for the (0 1 1) state. Both states are almost in the same energy region, about 4300 cm^{-1} above the zero point energy. For the bend and asymmetric stretch mode, it appears that the

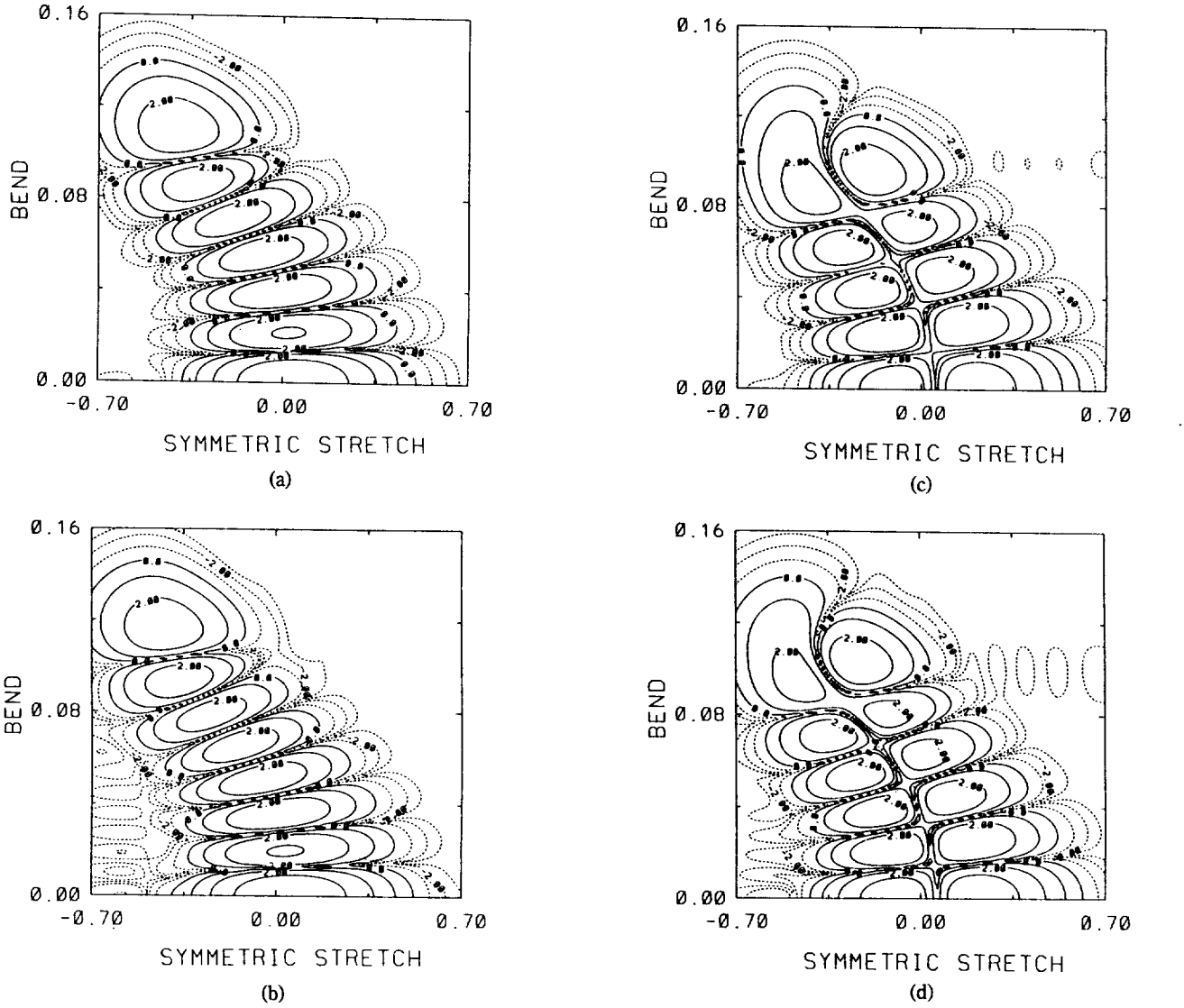

Figure 5. Contour plots of the square of the wavefunctions of the (a) (0 6 0) (b) (0 7 0) (c) (1 4 0) (d) (1 5 0) state for the model potential function. The nodes are clearly visible along the bend and symmetric stretch coordinate. Values of common logarithm are plotted with contour interval of 1.0, which is same in Figure 6 and Figure 7. Dotted lines represent the negative values.

effects of kinetic vibrational mode coupling on total energy is more noticeable in combination levels compard to the levels of pure vibrational mode in the same energy region. This is evident when we compare the effect of the vibrational coupling for the (0 6 0), (0 0 2), and (0 3 1) states which show the energy increase of 197, 253, and 408 cm^{-1} above the zero point energy differences between H_0 and H, respectively. These states are almost in the same region of energy (about 7000 cm^{-1} above the zero point energy).

One may be inclined to consider that our results were caused due to the simplicity of the model potential function used in obtaining energies of the molecule. To compare our results for the model potential function with the results for the real molecule, same vibrational calculations for CH_2^+ were carried out with the real, SPF type expanded potential function of the molecule described in Sec. III. In Table 3, we show the results for the real molecule of CH_2^+ which has about the same height of potential barrier to linearity as the model potential function. The results for real molecule of CH_2^+ show a similar mode selectivity in the effect of kinetic vibrational coupling on total energy as the results for model potential, although the magnitudes of coupling effects are somewhat different. For example, in real molecule of CH_2^+, the coupling energy increases rather slowly in the levels of pure bend mode as the levels go up, and negative coupling effect on total energies which appeared in the levels of pure symmetric stretch mode in case of the model potential are not shown above (1 0 0) level. The differences in magnitude between the results of model and real potential function could be attributed to the oversimplified expansion of the model potential function in the vibrational coordinates, especially in the asymmetric stretch coordinate. The differences also can be analyzed in terms of mode mixing in vibrational motion in higher energy states. In real molecule of CH_2^+, it was found that the mixing of symmetric stretch and bend mode in highly excited states is much heavier than in case

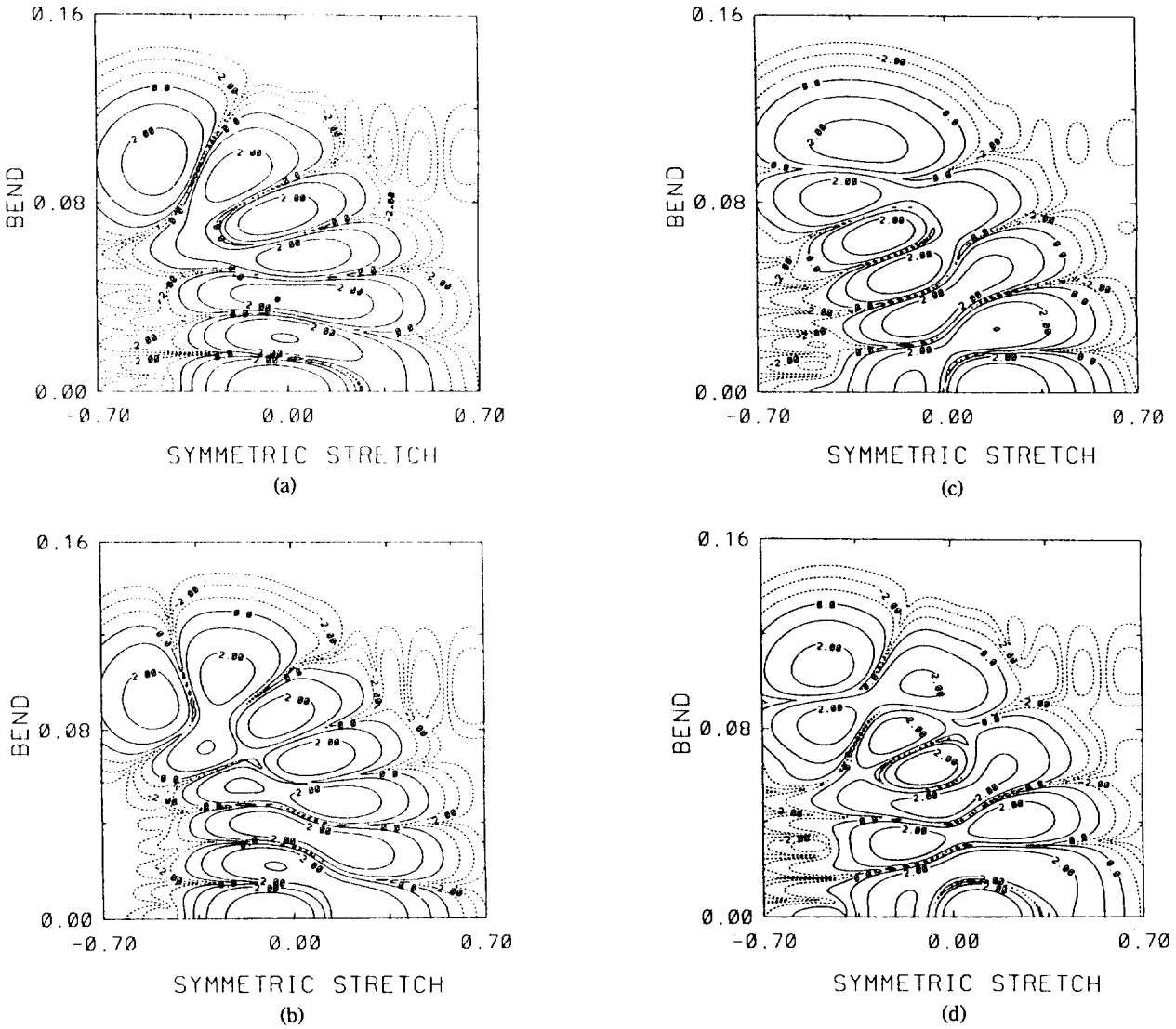

Figure 6. Contour plots of the square of the wavefunctions of the (a) thirteeth (b) eighteenth (c) fourteenth (d) nineteenth state above the ground state for nuclear singlet with $J=0$ in real molecule of CH_2^+. The mixing of the bend and symmetric stretch mode makes the vibrational assignment difficult. These states would be assigned as (0 6 0), (0 7 0), (1 4 0), and (1 5 0) state, respectively.

of the model potential. In Figure 5 and Figure 6, we plot the contours of the wavefunctions for (0 6 0), (0 7 0), (1 4 0), and (1 5 0) levels for the model and real potential function, respectively. In these figures, the values of the probability density of the wavefunction integrated over asymmetric stretch coordinate and rotational angles were plotted in the symmetric stretch and bend coordinate. While the nodes are clearly visible for the states in case of the model potential function, the strong mixing between the symmetric stretch and bend mode in real molecule of CH_2^+ makes it difficult to assign these vibrational states correctly. The mixing of symmetric stretch mode into the levels of bend has an effect of reducing the kinetic vibrational coupling energy in these levels, and the reverse is true for the levels of symmetric stretch mode mixed with the bend mode.

To investigate the effect of the kinetic vibrational coupling terms on wavefunctions and broken nodal structure in real molecule of CH_2^+, we plot the contours of the wavefunctions obtained from the unperturbed Hamiltonian (H_0) for the corresponding states in Figure 7. Although the nodal structure develops clearer in Figure 7, it is shown that these contours are not much different from the ones in Figure 6, where the wavefunctions obtained from full Hamiltonian (H) were plotted. This indicates that the broken nodal structure and chaotic behavior in molecular motion for CH_2^+ are caused primarily by the vibrational mode coupling in the potential energy function rather than coupling in the kinetic energy operator for the states with $J=0$.

Summary and Conclusion

We have found that inclusion of vibration-rotation interaction terms in Hamiltonian increases the total energies for all the levels of zero total angular momentum in a quasilinear symmetric triatomic H-C-H system with the model potential function as expected. However, the extent of the in-

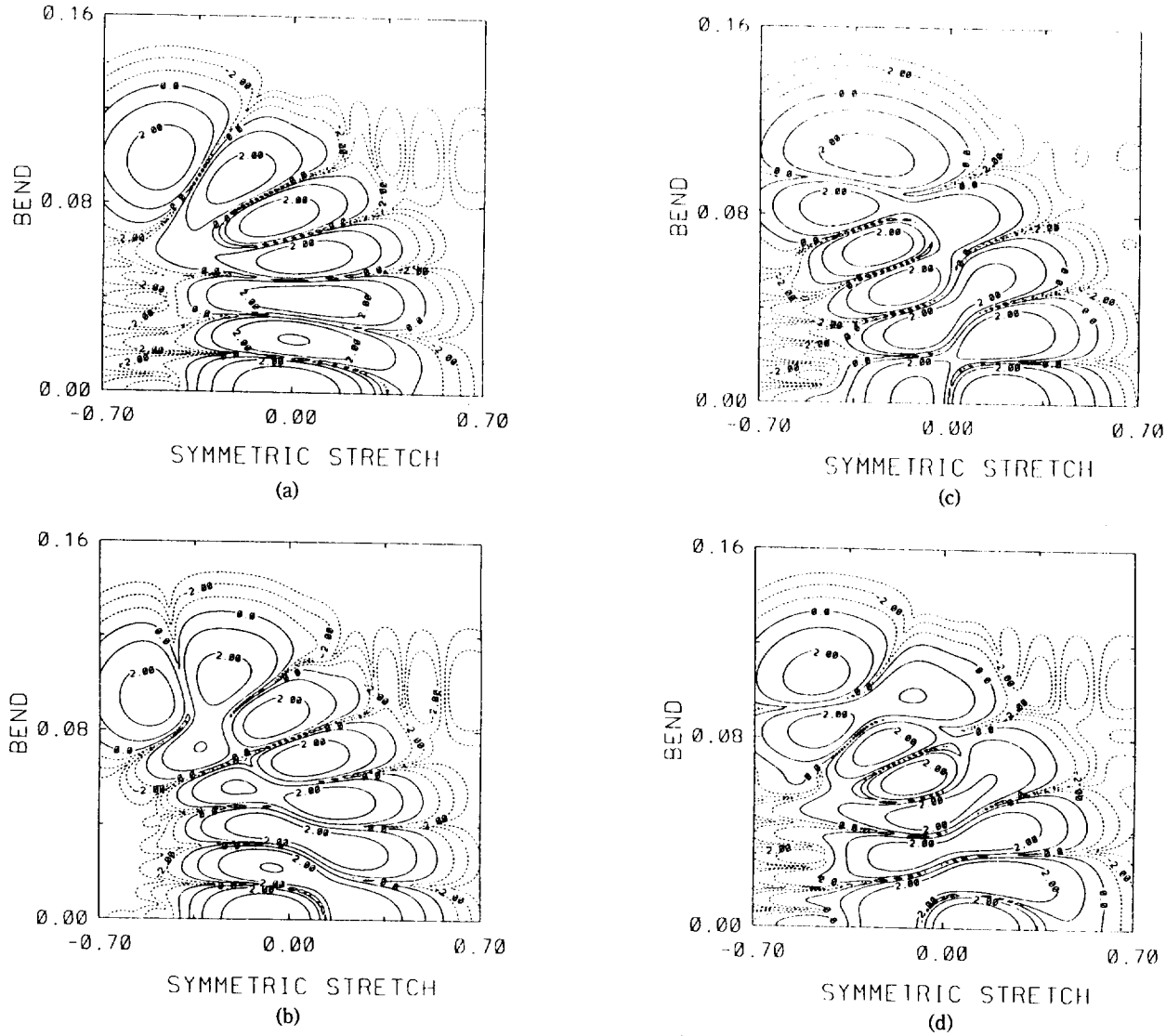

Figure 7. Contour plots of the square of the wavefunctions of the (a) thirteenth (b) eighteenth (c) fourteenth (d) nineteenth state above the ground state for nuclear singlet with $J=0$ in CH_2^+ without vibration-rotation interaction. The nodal structure is slightly better than in Figure 6.

crease of coupling energies in excited levels is strongly dependent upon the specific vibrational modes of the levels involved. While the difference between the energies with and without vibration-rotation interaction terms becomes larger for the levels of asymmetric stretch and bend mode as the total energies of the molecule increase, it becomes smaller for the excited levels of symmetric stretch mode. The results for the real molecule of quasilinear CH_2^+ show the similar dependence on vibrational mode, although the magnitudes of coupling energies are different from the results for the model potential function. The disagreement between the results for the real and model potential function and the disappearance of (negative) coupling effect in the excited levels of pure symmetric stretch mode for real CH_2 could be understood in terms of heavy mode mixing between symmetric stretch and bend mode in excited vibrational states. It is shown that the mode mixing and the broken nodal structure of CH_2^+ in highly excited levels for $J=0$ are mainly caused by the vibrational coupling terms in potential energy operator rather than kinetic energy operator. This, of course, is true only if the vibronic interaction like Renner-Teller effect[15] is not significant. It appears that the potential barrier has an effect to reduce the kinetic vibrational coupling energy for (0 1 0) level in real molecule of CH_2^+. This suggests that the vibration-rotation coupling energies could be smaller as the levels go up for excited levels of pure bend mode as well as symmetric stretch mode with $J=0$ for triatomic molecules with significant potential barriers to linearity. Overall, our results would serve as a salutary warning against the conventional notion that vibration-rotation coupling energy will be larger in higher energy levels than in lower levels. Our study also shows that the model potential function employed in this study could be used effectively for further modelization of the potential energy surfaces of the general triatomic molecules with arbitrary barrier to linearity from the equilibrium bent configuration. The effect of barrier

height and molecular rotation (non zero angular momentum) on vibrational mode mixing in triatomic molecules is under investigation.

Acknowledgment. The author thanks Professor Don Secrest of University of Illinois at Urbana-Champaign for several helpful discussions and his kindness to allow me to use Cray Y-MP supercomputer in National Center for Supercomputing Applications(NCSA) on his account. This work was supported in part by the grant from the Korea Science and Engineering Foundation.

References

1. Yamanouchi, K.; Takeuchi, S.; Tsuchiya, S. *J. Chem. Phys.* **1990**, *92*, 4044.
2. Deleon, A.; Jost, R. *J. Chem. Phys.* **1991**, *95*, 5686.
3. Heller, E. J. *J. Chem. Phys.* **1990**, *92*, 1718.
4. Tennyson, J.; Henderson, J. R. *J. Chem. Phys.* **1989**, *91*, 3815.
5. Bačić, Z.; Light, J. C. *J. Chem. Phys.* **1986**, *85*, 4594.
6. Chang, B. H.; Secrest, D. *J. Chem. Phys.* **1991**, *94*, 1196.
7. Natanson, G. A. *J. Chem. Phys.* **1990**, *93*, 6589.
8. Estes, D.; Secrest, D. *Mol. Phys.* **1986**, *59*, 569.
9. Lee, J. S. *J. Chem. Phys.* **1992**, *97*, 7489.
10. Bartholomae, R.; Martin, D.; Sutcliffe, B. T. *J. Mol. Spectrosc.* **1981**, *87*, 367.
11. Simons, G.; Parr, R. G.; Finlan, J. M. *J. Chem. Phys.* **1973**, *59*, 3229.
12. Lee, J. S.; Secrest, D. *J. Phys. Chem.* **1988**, *92*, 1821.
13. Lee, J. S.; Secrest, D. *J. Chem. Phys.* **1986**, *85*, 6565.
14. Lee, J. S.; *Ph. D. Thesis*, University of Illinois at Urbana-Champaign: Urbana, Illinois, U. S. A., **1986**.
15. Renner, R. Z. Physik **1934**, *92*, 172.

Crystal Structures of Fully Dehydrated Zeolite Cd_6-A and of $Rb_{13.5}$-A, the Product of its Reaction with Rubidium, Containing Cationic Clusters

Se Bok Jang, Yang Kim, and Karl Seff*

Department of Chemistry, Pusan National University, Pusan 609-735
**Department of Chemistry, University of Hawaii, 2545 The Mall Honolulu, Hawaii 96822-2275, U.S.A.*
Received October 25, 1993

The crystal structures of Cd_6-A evacuated at 2×10^{-6} Torr and 750℃ ($a=12.216(1)$ Å), and of the product of its reaction with Rb vapor ($a=12.187(1)$ Å), have been determined by single-crystal x-ray diffraction techniques in the cubic space group $Pm\bar{3}m$ at 21(1)℃. Their structures were refined to the final error indices, $R_1=0.055$ and $R_2=0.067$ with 191 reflections, and $R_1=0.066$ and $R_2=0.049$ with 90 reflections, respectively, for which $I>3\sigma(I)$. In dehydrated Cd_6-A, six Cd^{2+} ions are found at two different threefold-axis sites near six-oxygen ring centers. Four Cd^{2+} ions are recessed 0.50 Å into the sodalite cavity from the (111) plane at O(3), and the other two extend 0.28 Å into the large cavity from this plane. Treatment at 250℃ with 0.1 Torr of Rb vapor reduces all Cd^{2+} ions to give $Rb_{13.5}$-A. Rb species are found at three crystallographic sites: three Rb^+ ions lie at eight-oxygen-ring centers, filling that position, and ca. 10.5 Rb^+ ions lie on threefold axes, 8.0 in the large cavity and 2.5 in the sodalite cavity. In this structure, ca. 1.5 Rb species more than the 12 Rb^+ ions needed to balance the anionic charge of zeolite framework are found, indicating that sorption of Rb^0 has occurred. The occupancies observed can be most simply explained by two "unit cell" compositions, Rb_{12}-A·Rb and Rb_{12}-A·2Rb, of approximately equal population. In sodalite cavities, Rb_{12}-A·Rb would have a $(Rb_2)^+$ cluster and Rb_{12}-A·2Rb would have a triangular $(Rb_3)^+$ cluster. Each of the atoms of these clusters must bind further through a six-oxygen ring to a large cavity Rb^+ to give $(Rb_4)^{3+}$ (linear) and $(Rb_6)^{4+}$ (trigonal). Other unit-cell compositions and other cationic cluster compositions such as Rb_8^{n+} may exist.

Introduction

Complete dehydration of fully Cd^{2+}-exchanged zeolite A had not been achieved. Cd_6-A evacuated at 500℃ and 2×10^{-6} Torr for 2 days contains three H_2O molecules per unit cell,[1,2] and temperatures as high as 700℃ had not been found to be sufficient to remove all water.[3]

During the past decade, a series of attempts to achieve full Rb^+-exchange of zeolite A had failed.[4,5] Seff *et al.* reported that large monovalent Rb^+ ions exchanged incompletely into zeolite A by flow methods.[4] Only eleven of the twelve Na^+ ions per unit cell were replaced by Rb^+.

Fully dehydrated, fully Rb^+-exchanged zeolite A has been prepared by the reduction of all of the Na^+ ions in dehydrated Na_{12}-A by rubidium vapor.[6] In a series of structures, 12.6 (2) to 13.5(2) Rb species were found per unit cell, more than the twelve Rb^+ ions needed to balance the anionic charge of the zeolite A framework. The structural analyses indicated that dirubidium or trirubidium clusters inside the sodalite cavity coordinate further to rubidium ions in the large cavity